

Accurate Estimation of Blood Glucose with HbA_{1c} Quantification by a Reliable Photo Acoustic Method

¹J. Sundararajan, ²V. Palanisamy and ¹Mandyam Sandeep

¹Paavai Engineering College, NH-7, Pachal, Namakkal-637 018, India

²GCT, Coimbatore, India

Abstract: Diabetes Mellitus, a disorder that results in abnormality of blood glucose levels, has been the rapidly growing disorder currently reported. Glucose, being one of the most important compound that is vital for the human body, should be maintained in correct levels. The right blood glucose level is important as it provides different parts of the body with energy to function properly. Diabetics must hence know their blood glucose levels, so that they can control them with supplements like oral drugs, other treatments or calisthenics. The measurement of the total glucose concentration is currently invasive and time consuming. The most popular method of glucose quantification is to estimate the glycated hemoglobin concentration. The glucose measurements are accurate in this method the reason being that the hemoglobin molecules pick up glucose in about the same proportion as the glucose that exists in the bloodstream. The photo acoustic technique of HbA_{1c} may provide accurate and non-invasive measurement of glycated hemoglobin concentration by probing blood vessels that in turn gives the total blood glucose concentration. In this research, we studied the influence of photo acoustic signals on the HbA_{1c}, an important constituent of the RBC (stable ketoamine adduct) and illustrate the results to compute the blood glucose levels. The results obtained by this method prove to be strikingly similar (highly efficient) compared to the standard *in-vitro* procedures. Further extension of this technique can be made to study the other blood components.

Key words: Photo Acoustic HbA_{1c} (PAH), stable ketoamine adduct, pulsed laser diode, photo acoustic signal strength

INTRODUCTION

The measurement of the total glycated hemoglobin concentration is the widely used blood test for quantifying glucose in normal as well as diabetic patients. The reason for this is the versatile nature of this molecule. The complications associated with diabetes are mainly due to the non-enzymatic glycation of proteins (Brownlee, 2000; McCance *et al.*, 1993; Thorpe and Baynes, 1996; Vlassara *et al.*, 1986). The Maillard hypothesis suggests that chemical modification of proteins by glucose and subsequent reactions of the adduct may result in products which are directly responsible for many pathological conditions in diabetes (Brownlee, 2000; Brownlee *et al.*, 1988; Vlassara *et al.*, 1992). The reaction of glucose with amino groups in proteins results in the reversible formation of a Schiff's base or aldimine, which can undergo irreversible Amadori rearrangement (Fig. 1) to form a ketoamine product. Glycation is also a process that appears to be associated with age-related disorders and may be particularly important in the context of long-

lived proteins which do not undergo rapid synthesis and turnover (Thorpe and Baynes, 1996; Reiser, 1988; Wautier and Guillausseau, 1998; Vitek *et al.*, 1994; Lyons *et al.*, 1991; Pande *et al.*, 1979; Fu *et al.*, 1994; Ledesma *et al.*, 1995; Makita *et al.*, 1992). The initial observation that hemoglobin was glycated *in vivo* (Allen *et al.*, 1958; Holmquist and Schroeder, 1966), specifically at the N-terminus of the L-chain, triggered a very large number of investigations on the non-enzymatic glycation of proteins *in vivo* and *in vitro*. The purpose of many such studies was the characterization of site-specificity of glycation and the factors catalyzing rearrangement to the Amadori product. At present, the technique for quantifying HbA_{1c} (glycated hemoglobin) concentration is invasive and cannot provide results rapidly. Here we propose to use a photo acoustic technique for non-invasive and accurate measurement of HbA_{1c} concentration.

The photo acoustic technique is based on the generation of a near infrared wave by pulsed laser diode and time-resolved detection of the acoustical wave by the acoustical transducer. It can be used for tissue

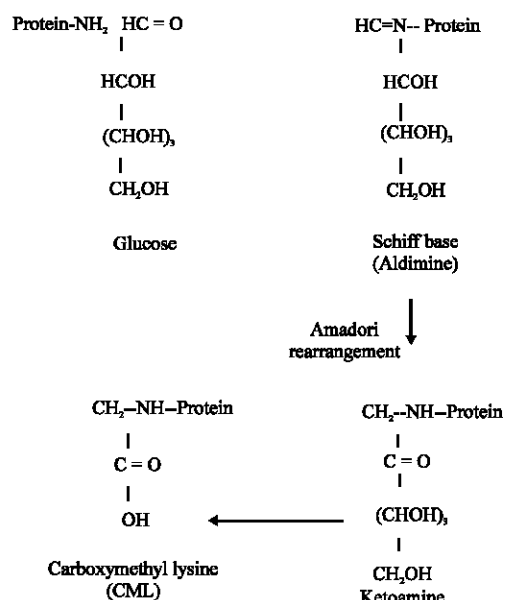


Fig. 1: Amadori rearrangement

characterization with high contrast (photo acoustic signal parameters are dependent on the optical properties of the irradiated tissue) and high resolution due to time-resolved detection of acoustic waves. Since Hemoglobin A1C (HbA_{1C}) is the post translational modification of glucose and hemoglobin, the major blood component, the photo acoustic technique is sensitive to variation of its concentration.

We studied the variation of HbA_{1C} concentration in blood, its behavior under photo acoustic signals, blood vessel diameter and photo acoustical transducer displacements on signals recorded in transmission and reflection models from a phantom of the radial artery. The outputs of this method were compared with those of the standard *in-vitro* techniques and they showed a very good acceptability range.

Choice of Hb_{A1C} for quantifying glucose concentration:

The glucose molecules in the blood attach themselves to many of the chemical compounds like hemoglobin, Low Density Lipoprotein (LDL's), serum proteins (like albumin) and many more. When it is in the free aldehyde form, it can react with the hemoglobin molecule within the red cells of blood to form an aldimine adduct as shown in the Fig. 1. But this is a reversible reaction in equilibrium with the blood glucose and hence this aldimine adduct is labile. However it can undergo a shift in the double bond to the second carbon in an "Amadori Rearrangement" (Seetharama and James) to form a ketoamine adduct as shown. This ketoamine adduct is an irreversible arrangement of the hemoglobin and glucose molecules.

The changes in the chemical bonds, particularly the double bonds involving the first and second carbon of glucose modify both the electronic transition and molecular vibration environments from those of free glucose and hemoglobin to those of the adducts. Therefore, the optical absorption spectra and the photo acoustic spectra of the free glucose and hemoglobin, the aldimine and the ketoamine are each sufficiently different to form the basis for spectroscopic determination of the amounts of each form present in the blood. Now HbA_{1C} is the most prevalent of the ketoamine adducts with the β chain of the hemoglobin, representing 5 to 6% of the total hemoglobin in persons without diabetics.

MATERIALS AND METHODS

The setup used in the experiments included a compact pulsed laser diode combination to give variable light waves varying from (600-1200) nm and delivering high peak power, an acoustical transducer, an amplifier and a notebook (laptop computer) for signal acquisition and processing. Electromagnetic energy covering a wavelength 1064 nm is directed into the tissue sample like through the forefinger. Portions of the energy after interacting with material within the sample volume are collected by the piezoelectric transducers which have a center frequency of 2 MHz. The energy portion carries information relating to source energy and the levels of labile and stable compounds within the sample volume, respectively. The portions are converted into electrical signals representative of the intensities of the respective portions in each of the multiplicity of wavelength bands. The block diagram of the setup is shown in Fig. 2.

The electrical signals are pretreated in accordance with known information to remove deviations from established reference conditions to form data signals that are a function of fractional portion of the energy in the wavelength bands absorbed and scattered by the material in the measurement volume. Selected group of the data signals are processed in accordance with the photo acoustic model. This model is developed from analysis of data signals together with known values of the analytes derived from measurements on a calibration set of samples larger in number than the number of wavelength bands included in the set of the selected group of data signals to develop analyte signals representative of the amount of HbA_{1C}. The analyte signals may be stored and displayed in a form suitable for medical use.

Design and instrumentation: The system for measuring biological parameter, HbA_{1C}, compresses the steps of

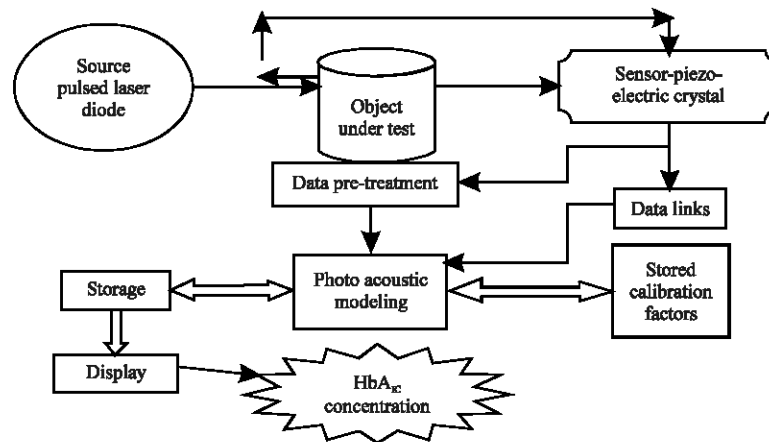


Fig. 2: Block diagram of the setup

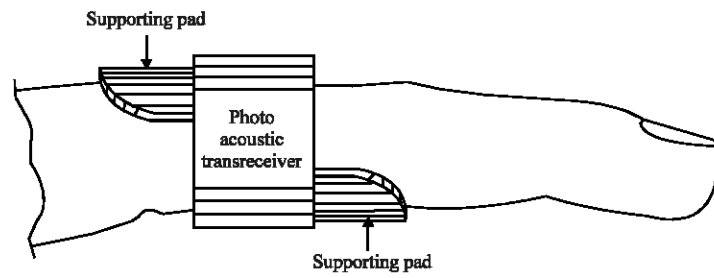


Fig. 3: Basic design for the technique in discussion

directing laser pulses [(700-1100) nm] from a pulsed laser diode (Thomas *et al.*, 2005; Beard *et al.*, 2004; Thomas *et al.*, 2006) into a body part consisting of soft tissue, such as the finger tip to produce a photo acoustic interaction. The resulting acoustic signal is detected by a transducer and analyzed to provide the hemoglobin A_{1c} parameter. The above Fig. 3 illustrates this.

Sensor model: In pulsed excitation of condensed matter, the application of microphones is hampered due to their restricted bandwidth. Therefore, piezoelectric transducers are employed in many cases for the detection of ultrasonic pulses in liquid and solid samples (Jackson and Amer, 1980; Nelson and Patel, 1981). Quartz crystals, Piezoelectric ceramics such as lead Zirconate Titanate (PZT) (Wu *et al.*, 1983), lead metaniobate and lithium niobate (Ogi *et al.*, 2002) as well as piezoelectric polymer films can be applied to the detection of laser-induced shock pulses (Tam, 1986). The most common piezoelectric polymer is Poly Vinylidene Fluoride (PVDF), which is available in different thicknesses ranging from 5-100 μm as a transparent film or coated with metals for electrical contact (Sessler, 1981). In the currently used pulsed PA analysis of the blood components through the skin, the

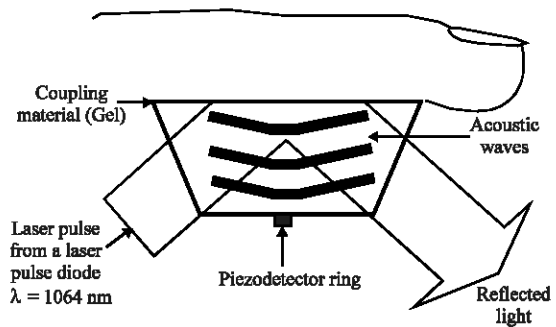


Fig. 4: Photo acoustic transducer

generated pressure pulses are often detected in backward mode, where excitation and detection are performed at the same side of the sample. Since piezoelectric transducers are generally not transparent, illumination through the piezo and detection at the same point are not possible. This has been overcome by using the sensor set-ups shown below. This PA sensor uses a transparent prism as coupling material for both illumination of the sample and transfer of the acoustic energy to the detector. The sample is eliminated through a transparent prism which also acts as an acoustic coupling material (Fig. 4).

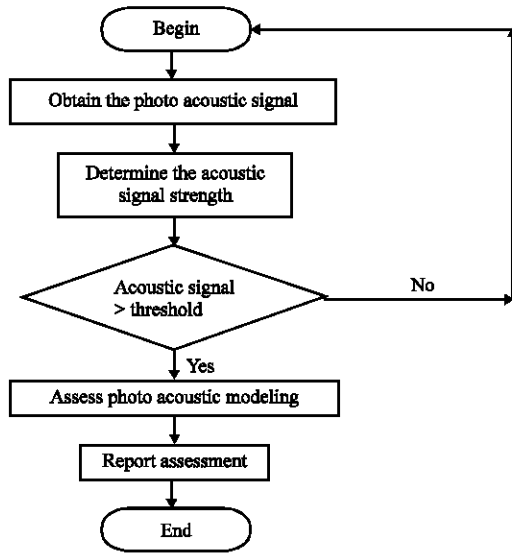


Fig. 5: Data pretreatment

Monitoring system: The user interface module preferably serves as a desktop environment or a user computer that enables the user to access and execute the photo acoustic model development and execution application via known data. The interface application is preferably configured to accept any conventional signal from a photo acoustic transducer that converts the acoustical pulses to electrical signals. Further more, the application is preferably configured to output a conventional output signal indicative of the predicted property (Fig. 5).

The memory is preferably an external memory and includes capacity to store a library of photo acoustic model for which the user is matched. The build model communicates the user model within the interface application in a bidirectional manner. From the user interface module, the build module receives user inputs to develop photo acoustic models. In return, the build model transmits to the user interface module information relevant to the model available for the development and details regarding the model themselves. At any time the user can save a model to the memory and access a model in the memory (Fig. 6).

Turning now to the real time module, the real time module communicates bidirectional with the interface application and more particularly with the process system interface. The real time module receives photo acoustic models of HB_{AIC} . The module applies selected photo acoustic spectra and generates a prediction property. The real time module generates data for the display to the user via the interface application.

Signal processing and analytical model: In the near infrared, the scattering coefficient of the skin is much larger than its absorption coefficient. A collimated light beam at normal incident on a sufficiently thick skin can be considered. Assuming that the scattering and absorbing centers are uniformly distributed and neglecting internal light generation by fluorescence, the optical distribution can be described by the stationary radiative transfer equation, when the duration of a light pulse is longer than 10-8 s.

$$s \cdot \Delta I(r, s) \approx \mu_e I(r, s) + \mu_e / 4\pi \int_{4\pi} P_f(s, s') I(r, s') d\omega' + (\mu_e / 4\pi) p_e(s, z) I_c(r, z)$$

The collimated light is attenuated according to modified Beer's law, i.e.,

$$dI_c(r, z) = -\mu_e I_c(r, z) \cdot dz,$$

Where $I_c(r, z)$ is the collimated intensity at the position r in the incident direction z and r is a position vector. $I(r, s)$ is the scattered specific intensity (watt/cm²/sr) at the position r in the direction s and s is the directional unit vector. $P_f(s, s')$ is the phase function that represents the scattering contribution from s' in the direction s . ω' is the solid angle μ_e is the extinction coefficient defined as the sum of the absorption coefficient μ_a and the scattering coefficient μ_s .

A powerful photo acoustic technique, to be precise the Time-Resolved Stress Detection (TRSD) can be used since it can rebuild the absorbed optical distribution by simultaneously detecting the laser induced stress amplitude. This can be used to measure the absorption and scattering coefficients together and to image the interior structure of turbid samples. The most common type of optical source in near-infrared TRSD is a pulsed Q-switched Nd: YAG laser. Short laser pulses allow the most efficient realization of PA generation at a given incident laser fluence. Since pressure is also an important factor the PA pressure of a planar PA source produced in a clear (non- scattering) absorbing medium by a short laser pulse (δ pulse) can be described by the equation

$$p_a(\tau) = \{E_0 \alpha \beta v^2 / 2C_p\} \{ \Theta(-\tau) \cdot \exp(-\alpha v_a \tau) + R_c \cdot \Theta(\tau) \exp(-\alpha v_a \tau) \}$$

$$p_t(\tau) = \{E_0 \alpha \beta v^2 / 2C_p\} T \cdot \Theta(\tau) \exp(-\alpha v_a \tau),$$

Where,

$$R_c = (\rho_t v_t - \rho_a v_a) / (\rho_t v_t + \rho_a v_a),$$

$$T = 2\rho_t v_t / (\rho_t v_t + \rho_a v_a),$$

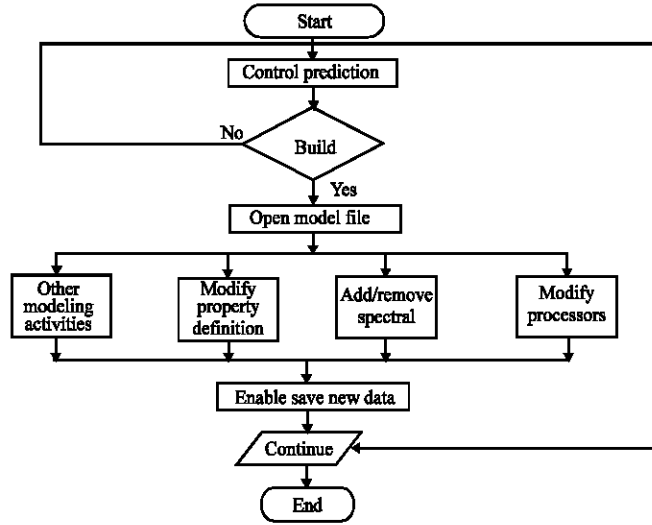


Fig. 6: Monitoring flow chart

$$\tau = t - (z/v_a),$$

$$\tau_t = t + (z/v_t),$$

Θ is the Heaviside unit function, ρ and v are the density and the acoustic velocity of the medium, respectively. The subscripts a and t describe the parameters in the absorbing and the transparent media.

At initial time ($t = 0$), when the laser incidents on the absorbing medium, Eq. 1 is simplified as

$$P(z) = (E_0 \alpha \beta v^2 / C_p) \exp(-\alpha z) = \Gamma E_0 \alpha \exp(-\alpha z)$$

But the tissues and cells cannot be considered as non-scattering medium and hence considering the reduced scattering coefficient of the tissues μ_s' to be much larger than its absorption coefficient μ_a the corresponding stress can be modified as

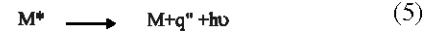
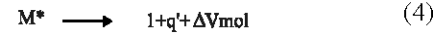
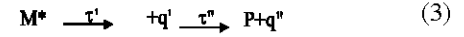
$$P(0) = \Gamma E(0) \mu_a(z=0)$$

$$P(z) = \Gamma E_0 \kappa_s \mu_a \exp(-\mu_{eff} z)$$

$$= (1/2) \Gamma E_0 \mu_{eff} [\exp(\mu_{eff} l^*) - \exp(-\mu_{eff} l^* (2\Delta + 1))] \exp(-\mu_{eff} z).$$

Where $z > (1/\mu_{eff})$

For optically thick samples, $E(0) = (1 + 7.1 R_d \infty) E_0$, where $R_d \infty$ is the total diffuse reflectance. κ_s is the factor that accounts for the effect of backscattered irradiance that increases the effective energy density absorbed in the subsurface.



$h\nu$ = Energy absorbed.
 ΔV_d = Volumetric change.
 τ, τ', τ'' = Time constants.
 P = Product after τ''
 q = Released heat
 $h\nu'$ = Released energy

We know

$$\chi = 1064 \text{ nm}$$

$$\tau = 10 \text{ ns}$$

The acoustical pressure generated is

$$P(r, t) = 1/4 \Pi c * \partial/\partial t \{ \int [P_0(r - \Delta v)/ct] ds \}$$

Where $P(r, t)$ is a function of radius and time.
 Also,

$$\partial^2/\partial t^2 P(r, t) - C^2 \nabla^2 P(r, t) = \partial/\partial t P_0(r) \partial(t)$$

Where

$$P_0(r) = B \beta / C_p F_0 \mu_a \exp[-z \mu_a f(x)]$$

$$\Delta r = ct$$

- t = 10ns (from above).
 c = Speed of sound 320 m sec⁻¹.
 C = Specific heat at constant volume.
 B = Bulk modulus (isothermal).

$$F(z) = F_0 \exp(-z\mu_a)$$

- z = Depth
 F₀ = Fluence at surface
 μ_a = Absorption

RESULTS AND DISCUSSION

The blood glucose concentration of a normal person ((6.5-8.5) % Hb_{A1C}) was previously measured with the *in-vitro* techniques like the HPLC test. The analysis of the blood glucose concentration of the same person gave the output plot as shown in Fig. 7. The input excitation pulse for the latter technique was varied for 3 wavelengths viz. 790, 960 and 1064 nm and corresponding acoustical amplitudes were together plotted. The peaks are shown for the different wavelength pulses in the following graph.

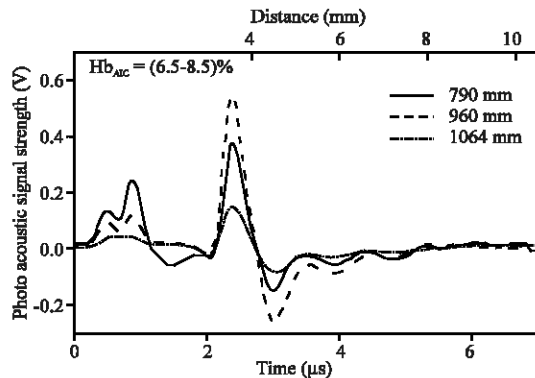


Fig.7: Blood glucose concentration

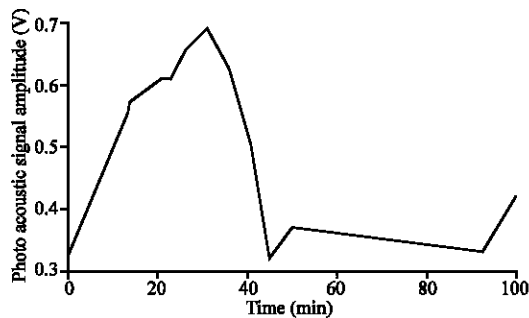


Fig. 8: Input excitation pulse-790 nm

The graph gives an implication of a low peak for 1064 nm input pulse excitation and a corresponding high one at 960 nm input pulse excitation. The above graph can be used to formulate a standard photo acoustic model of the HbA_{1C} molecule (stable Amadori rearranged ketoamine adduct).

Determination of HbA_{1C} concentration from the obtained

Signals: The following Fig. 8-10 show the time course of the photo acoustic signal amplitudes as the hemoglobin glycation varied in the RBC. Variation of the glycated hemoglobin concentration resulted in changes in the blood glucose and in changes in the photo acoustic signal amplitudes at 790 and 1064 nm. The variation of the signal amplitude at 790 nm is shown in the Fig. 8 while that at the input wavelength of 1064 nm is shown in Fig. 9. The resultant HbA_{1C} concentration was determined from the photo acoustic output variation and when plotted on a single sheet gave the graph shown in Fig. 10.

Comparison with a standard *in-vitro* technique: The HPLC test is one of the commonly followed *in-vitro* techniques for blood glucose determination. The following graph shows the result comparison of the above technique with the standard HPLC test (Fig. 11).

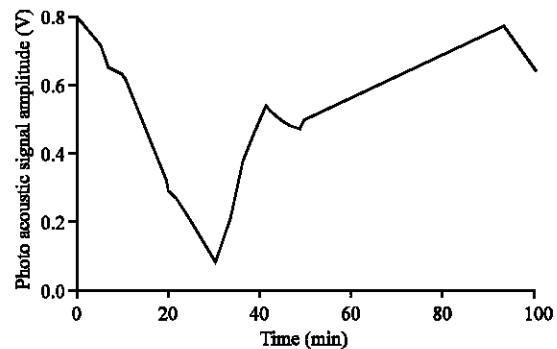


Fig. 9: Input excitation pulse-1064 nm

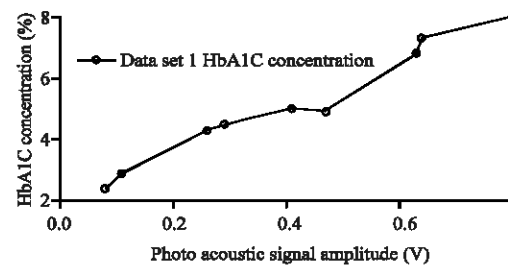


Fig. 10: Photo acoustic signal strength vs HbA_{1C} concentration